Settlement of the Kansai International Airport Islands

G. Mesri, M.ASCE[1]; and J. R. Funk, S.M.ASCE[2]

Abstract: The Kansai International Airport was constructed in Osaka Bay in 18- to 20-m-deep seawater to avoid noise pollution and land acquisition disputes. Construction of the 511-ha Island I began in 1987 and Runway I began operation in 1994. Construction of the 545-ha Island II began in 1999, and Runway II began operation in 2007. Using more than 2.2 million vertical sand drains fully penetrating into the 17.3- to 24.1-m-thick Holocene clay layer and 430 million cubic meters of fill material, the project is viewed as an engineering marvel. On the basis of a detailed review of the geology of Osaka Bay, construction of the Airport Islands, and the permeability and compressibility of the Holocene and Pleistocene subseabed deposits that reached a depth of 400 m below the seafloor at the Kansai Airport site, settlement analyses were conducted assuming the uniqueness of end-of-primary void ratio–effective vertical stress relationship and the C_α/C_c law of compressibility. Airport Island I has already settled below the 4-m above sea level surface elevation required by the design specification, and the surface elevation of Island II is predicted to be 4 m above sea level by 2023–2036. Airport Islands I and II will be at sea level, respectively, by 2067 or sooner and by 2058–2100. By the end of the 21st century, Island I and Island II are predicted to settle, respectively, 17.6 and 24.4 m. **DOI: 10.1061/(ASCE)GT.1943-5606.0001224.**

Author keywords: Kansai Airport; Osaka Bay; Offshore reclamation; Holocene and Pleistocene clay deposits; Pleistocene sand deposits; Primary and secondary settlements.

Introduction

Japan's extensive reclamation history stems from a need for additional land in coastal areas (Mikasa and Ohnishi 1981; Sasaki et al. 1987). Reclamation has taken place in Osaka Bay at least as early as the Edo era (1600–1867), when it was used for rice cultivation.

The Kansai International Airport was constructed 5 km off the coast of Senshu in 18- to 20-m-deep seawater to avoid noise pollution and land-acquisition disputes that were experienced at the Itami and Narita airports. Construction of Island I began in 1987, and Runway I began operation in 1994. Construction of Island II began in 1999, and Runway II began operation in 2007 [Nakase 1987; New Kansai International Airport Company (NKIAC) 2012].

As a part of the original design considerations, the surface elevation of the Kansai Airport islands were to remain above +4-m chart datum level (CDL) to avoid the erosive action of waves overtopping the seawall (Arai 1991). As of December 2012, the average seabed settlement has exceeded 12.9 and 14.2 m, respectively, for Airport Islands I and II (NKIAC 2012).

The Kansai Airport project has received considerable attention in the geotechnical engineering literature in part because of the scale of the project; Island I is 511 ha in approximately 18-m-deep seawater and Island II is 545 ha in approximately 20-m-deep seawater. The project is also significant because of the sufficiently detailed subseabed information and observations of settlement and pore-water pressure reaching depths up to 350 m below the seabed. The projected or observed consolidation behavior of the subseabed has been used in an ongoing debate on the uniqueness (Mesri and Choi 1985b; Mesri et al. 1995) of the end of primary (EOP) void ratio–effective vertical stress relationship of clay and silt deposits. Hight and Leroueil (2003) claimed that the Kansai reclamation project confirms that, under a given effective stress, the in situ strain, and thus settlement, is larger than that deduced from laboratory tests, thus concluding that a settlement analysis based on the assumption of uniqueness will lead to an underestimate of settlement resulting from primary consolidation. Rocchi et al. (2006), attributing observations in the Osaka Bay to an unusual settlement behavior of clays, stated that the field behavior of Osaka clays at these two sites demonstrates that primary compression settlements predicted by conventional interpretation of oedometer tests may be substantially lower than observed, casting doubt on the uniqueness of the EOP void ratio–effective stress relationship, which is found to provide reliable predictions only under special circumstances.

Mimura and Jang (2005) proposed that the phenomenon taking place because of the reclamation project is far from the conventional concept of consolidation in which deformation is primarily caused by dissipation of excess pore-water pressure. Imai et al. (2005) highlighted the confusion in connection to consolidation behavior of Osaka Bay Pleistocene clays by stating that "The most shocking finding is that a large compression endlessly takes place for [a] long time even when an applied load is smaller than p_c [preconsolidation pressure]. Why does such abnormal behavior take place?" In connection to modeling of consolidation characteristics of clays for settlement prediction of Kansai International Airport, Kobayashi et al. (2005) reported compression of a specimen of Ma3 clay subjected to a consolidation pressure in the recompression range, commenting that settlement continued "without showing a tendency of decreasing coefficient of secondary compression. . . . No definite answer for such large settlement under the overburden pressure can be given and this point needs more investigation in the future."

In this paper, detailed settlement analyses are reported for the Kansai Airport islands, based on the assumption of the uniqueness of

[1]Ralph B. Peck Professor of Civil Engineering, Dept. of Civil and Environmental Engineering, Univ. of Illinois at Urbana–Champaign, Urbana, IL 61801 (corresponding author). E-mail: gmesri@illinois.edu

[2]Geotechnical Staff, Shannon & Wilson, Inc., 1321 Bannock St., Seattle, WA 98103.

Note. This manuscript was submitted on February 12, 2014; approved on September 19, 2014; published online on October 30, 2014. Discussion period open until March 30, 2015; separate discussions must be submitted for individual papers. This paper is part of the ***Journal of Geotechnical and Geoenvironmental Engineering***, © ASCE, ISSN 1090-0241/04014102 (16)/$25.00.

the EOP e-σ'_v relationship of Holocene and Pleistocene Osaka Bay clays, together with the C_α/C_c law of compressibility for evaluating secondary compression and associated settlements (Funk 2013).

Geology of Osaka Bay

Osaka Bay, located in the western part of Osaka Basin at the eastern end of the Seto Inland Sea in southwest Japan, is bordered by the Rokko Mountains to the north, the Ikoma and Kongo Mountains to the east, and the Izumi Mountains to the south. Osaka Basin formed as a result of crustal movements that started in the Middle Miocene epoch, caused by the subduction of the Philippine Sea Plate beneath the Eurasian Plate (Inoue et al. 2003). The subseabed sediment profile and lateral variation of thickness for individual layer formations within Osaka Bay are a result of changes of global climate and relative sea level, as well as volcanic activity that occurred during the late Cenozoic era. The maximum depth to bedrock in Osaka Bay is more than 3,000 m near the center of the bay as shown in Fig. 1.

Osaka Basin began to subside and accumulate the lower part of the Osaka Group at the close of the Pliocene (Itihara et al. 1975). The subseabed sediment profile at the Kansai International Airport site, located in the southern portion of Osaka Bay, is shown in Fig. 2. The profile includes Pleistocene marine clay layers Ma0–Ma12 and Holocene marine clay layer Ma13. Marine clay layers alternate with sand layers Ds1 through Ds10 and nonmarine clays Doc and NMC, as well as very thin volcanic ash deposits not shown in Fig. 2.

The depositional environment, lateral continuity, and age of the Osaka Group sediments are constrained by more than 50 volcanic ash layers (Inoue et al. 2003). At the Kansai Airport site, the 1 million years before present (YBP) Pink volcanic ash is found between Ma1 and Ma2, the 0.85 million YBP Azuki ash is found in the lower portion of Ma3, the 0.30 million YBP Kkt ash is found in Ma10, the 0.23–0.25 million YBP Ata-Th is found in Ma11, the 20,000 YBP At is found in Ds1, and the 6,300 YBP K-Ah is found in Ma13 (Itihara et al. 1975; Nakaseko et al. 1984; Itoh et al. 2000, 2001).

Construction of the Kansai Airport Islands

In April 1968, the Ministry of Transportation (MOT) of Japan began surveying two onshore and six offshore sites for airport construction (NKIAC 2012). It was decided in 1974 that an airport 5 km off the coast of Senshu would avoid noise-related problems and land-acquisition disputes (Nakase 1987; Arai 1991; Tabata and Morikawa 2005).

Construction of the Kansai Airport Islands was an enormous undertaking. Approximately 180 million cubic meters of reclamation fill material was used to construct the 511-ha Island I and approximately 250 million cubic meters of reclamation fill material was used to construct the 545-ha Island II. The construction of each airport island consisted of four stages: (1) installation of vertical sand drains in the Ma13 clay layer following placement of a sand blanket on the sea floor, (2) construction of the seawall around the reclamation site, (3) reclamation of the airport island, and (4) construction of airport facilities.

Before installation of vertical sand drains, a 1.5-m-thick sand blanket was placed on the seafloor [Kansai International Airport Land Development Company (KALD) 2005]. Forty-centimeter-diameter displacement type vertical sand drains were installed to fully penetrate the Holocene marine clay layer Ma13 and form a drainage connection to the overlying sand blanket and the underlying sand layer Ds1. The vertical drains were installed on a 2.5-m-square pattern beneath the reclamation area for both Island I and Island II (Nakase 1987; Maeda et al. 1990; Arai 1991; Tabata and Morikawa 2005). Approximately 1 million sand drains were installed for Island I construction and 1.2 million sand drains were installed for Island II construction.

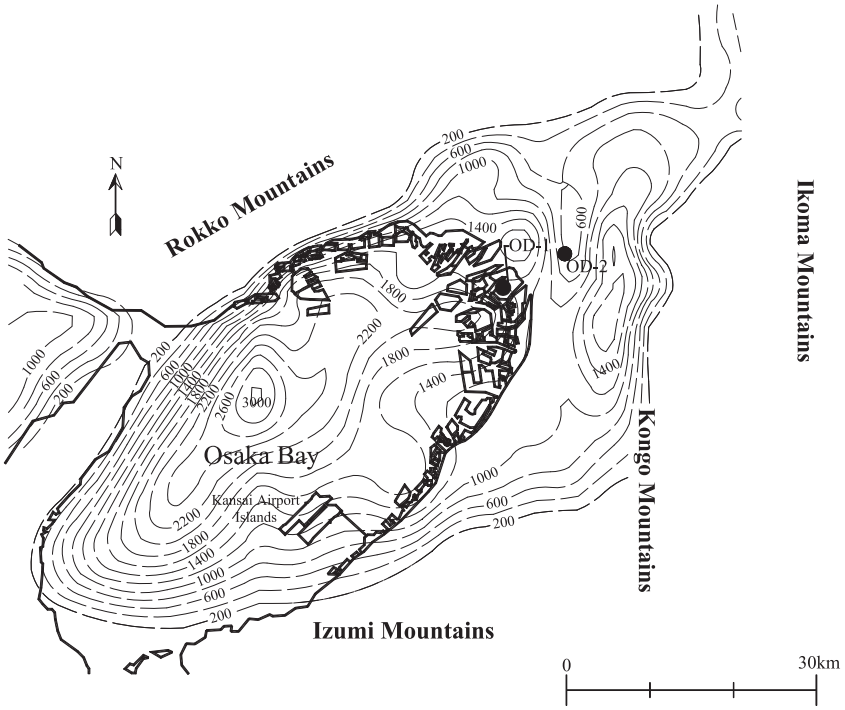

Fig. 1. Osaka Bay (data from Mikasa and Ohnishi 1981; Yamasaki and Nakada 1996; Sekiguch and Aksornkoae 2008) together with depth to bedrock contours in meters (data from Kagawa et al. 2004)

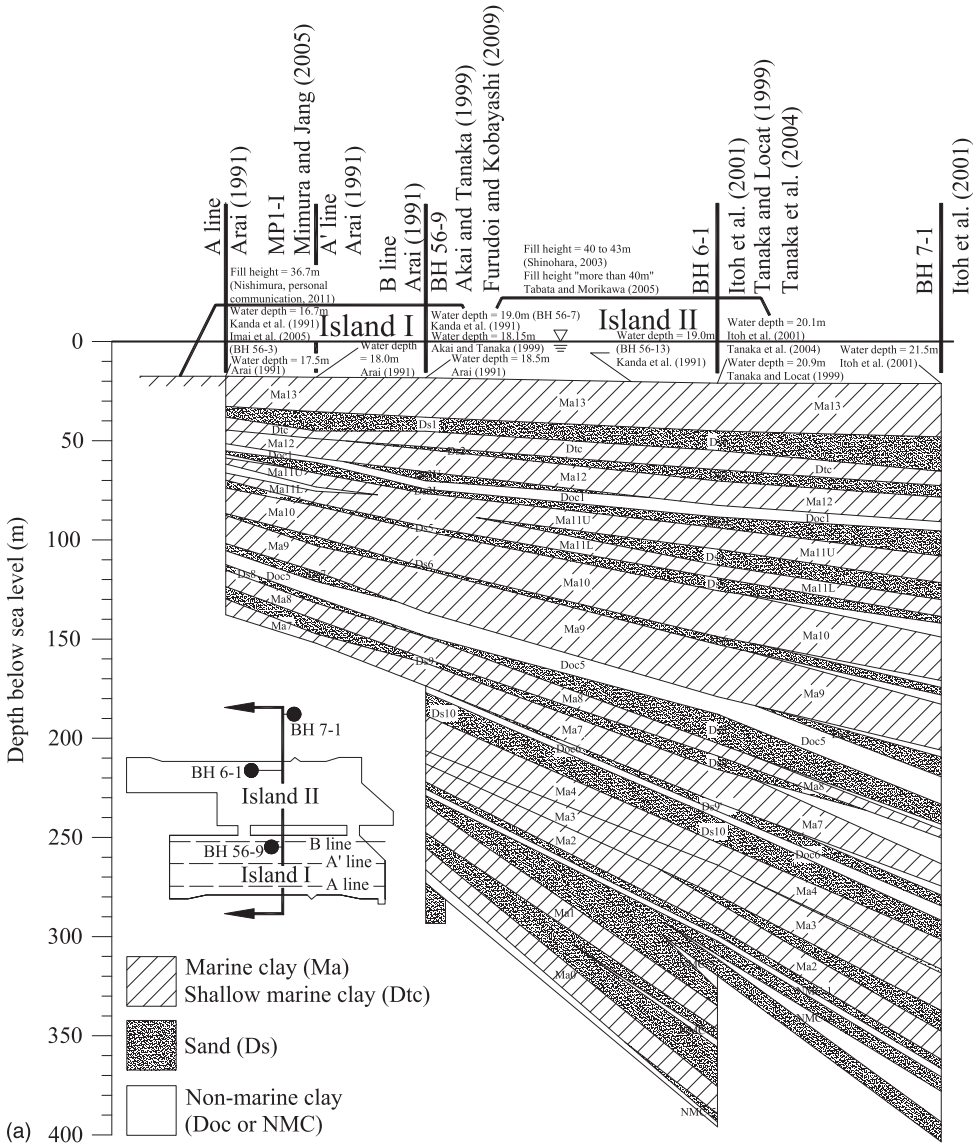

Fig. 2. (a) Subseabed profile at the Kansai International Airport site (10:1 vertical to horizontal exaggeration); (b) subseabed profile at the Kansai International Airport site (10:1 vertical to horizontal exaggeration)

The reclamation fill with a maximum particle size of 300 mm (Tabata and Morikawa 2005; Furudoi 2010) was obtained from Misaki, Kada, Tsuna, and Sumoto, located 10–30 km from the Kansai Airport site. The total unit weight of reclamation fill above water was in the range of 19.6−22.8 kN/m^3, and submerged unit weight of fill below water was in the range of 11.8−12.4 kN/m^3 (Arai 1991; Endo et al. 1991; Yamane et al. 2003; KALD 2005; Tabata and Morikawa 2005; Funk 2013).

Nakase (1987) reported the planned height of reclamation fill above the seafloor to be 30 m for Island I. Arai (1991) reported that fill height was increased to 33 m to accommodate settlement forecasts, and Nishimura (N. Nishimura, personal communication, 2011) reported the final height of reclamation fill above seafloor for Island I to be 36.7 m. For Island II, the height of reclamation fill above seafloor was reported by Shinohara (2003) to be 40–43 m and by Tabata and Morikawa (2005) and Furudoi (2010) as "more than 40 m."

The present settlement analyses were carried out for five locations on the airport islands, where detailed settlement and pore-water pressure observations were available. The load applied to the sea floor by the reclamation process has previously been either computed using the unit weight and thickness of the fill, taking into account the submergence effect (Shibata and Karube 2005; Kobayashi et al. 2005; Tabata and Morikawa 2005; Furudoi and Kobayashi 2009; Furudoi 2010; N. Nishimura, personal communication, 2011), or load cell measurements at the seafloor (Tabata and Morikawa 2005; Kobayashi et al. 2005; Furudoi 2010; N. Nishimura, personal communication, 2011). The reported seafloor reclamation loads are shown subsequently together with settlement and pore-water pressure observation and present predictions. Although the load cell measurements for MP2-II are relatively consistent, reaching a maximum value equal to 540 kPa, the load cell measurements for MP1-II were 485 kPa measured by Load Cell 1 and 640 kPa measured by Load Cell 2 in April 2008.

The decrease in reclamation load associated with settlement and the resulting submergence of reclamation fill below sea level are important considerations for settlement analyses of Kansai Airport because of the large seabed settlements. The reported reclamation loads, however, reach relatively constant values during the period of observation. According to M. Kobayashi (personal

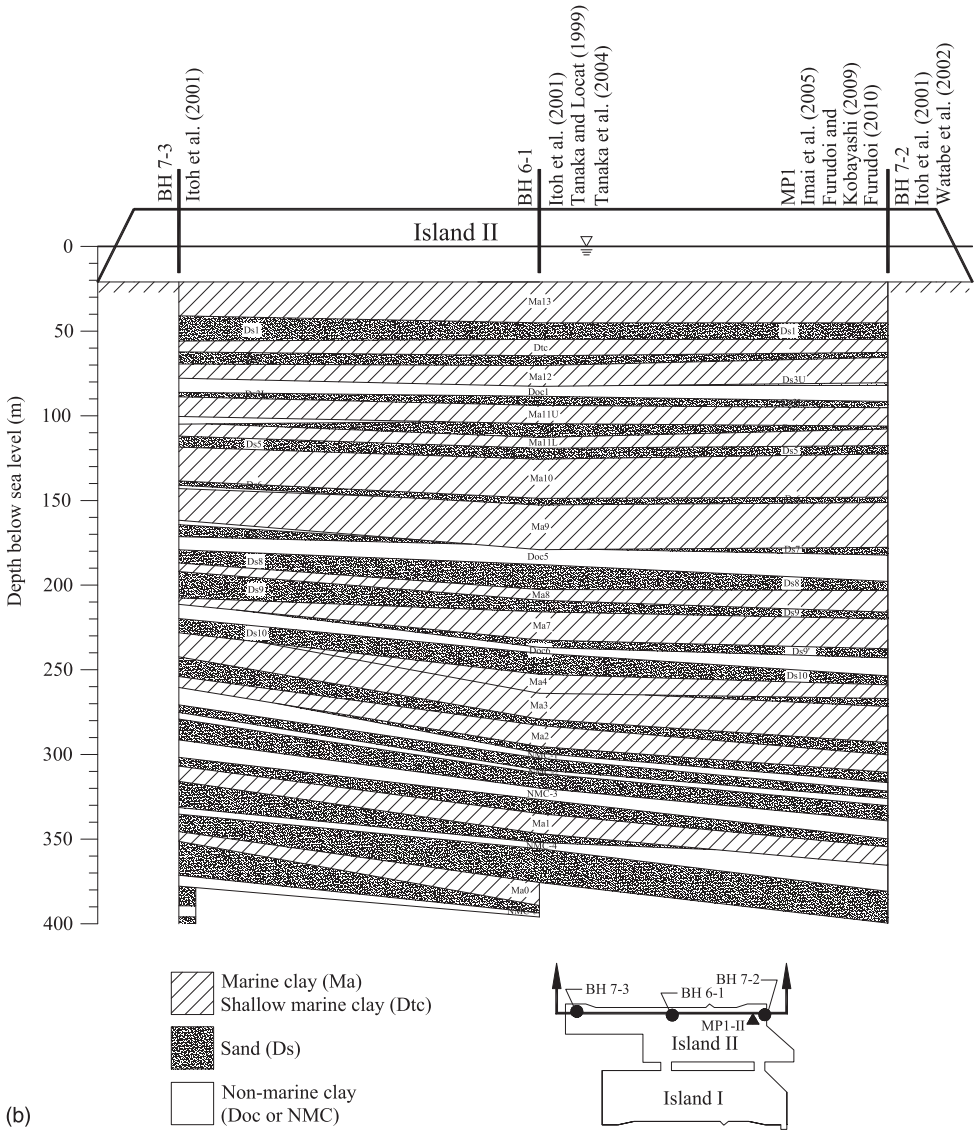

Fig. 2. (*Continued*.)

communication, 2007), the reported reclamation loads reach a constant value because reclamation fill was added in small steps even after the main reclamation was completed. This is evidenced by the load cell measurements between July 2004 and January 2010 at MP1-II. However, in the present settlement analyses, subsequent to January 2010, the reclamation load at the seafloor was reduced with time according to the submergence effect of airport settlement.

Calculated reclamation load at seafloor versus time reported by Furudoi and Kobayashi (2009), Furudoi (2010), and Shibata and Karube (2005) was used in the present settlement analyses at CT, K-I, and MP1-I, respectively. The average of the reported load cell measurements versus time at the seafloor was used for the present settlement analyses at MP1-II and MP2-II.

Permeability and Compressibility of Subseabed Deposits at the Kansai Airport Site

The initial subseabed investigation for the Kansai International Airport project began in 1977. Sixty-three borings were made to seabed depths ranging from 100 to 200 m, and two borings, one on the offshore side of Island I and one on the sea side of Island II, were made to a seabed depth of 400 m. Four additional 400-m-deep borings were made in 1994 and 1995 (Nakase 1987; Tabata and Morikawa 2005; Furudoi and Kobayashi 2009).

The subseabed stratigraphy across the Kansai Airport site, shown in Fig. 2, was constructed based on borehole data reported in the literature (Arai 1991; Akai and Tanaka 1999; Tanaka and Locat 1999; Itoh et al. 2001; Tanaka et al. 2004; Imai et al. 2005; Mimura and Jang 2005; Furudoi and Kobayashi 2009; Furudoi 2010). The seawater depth, referenced to CDL, increases gradually with distance from the shoreline and is approximately 17.0 m at the onshore side of Island I, 20.0 m at the offshore side of Island II, and 21.5 m into Osaka Bay, approximately 1 km from the offshore side of Island II (Arai 1991; Kanda et al. 1991; Akai and Tanaka 1999; Tanaka and Locat 1999; Itoh et al. 2001; Tanaka et al. 2004; Imai et al. 2005).

Representative values of index properties, including natural water content, Atterberg limits, clay-size fraction, and activity, are listed in Table 1. The water content and Atterberg limit values in Table 1 represent the average of all available data at the Kansai Airport site and are used for subsequent settlement analyses at MP1-I and MP2-II. Values specific to MP1-II were used for subsequent settlement analysis at MP1-II.

Table 1. Representative Values of Soil Properties for Each Sublayer

Layer	Sublayer	w_o (%)	w_p (%)	w_l (%)	I_p (%)	CF[a] (%)	A_c	σ'_p/σ'_{vo}	e_o	k_{vo} (m/s)	C_k
Ma13	1	110	35	102	67	45	—	2.10	2.933	2.3×10^{-8}	1.5
	2	96	35	99	64	45	—	1.60	2.560	1.1×10^{-8}	1.3
	3	86	32	90	58	45	—	1.50	2.293	5.0×10^{-9}	1.1
	4	74	30	78	48	45	—	1.50	1.973	2.2×10^{-9}	1.0
	5	66	30	66	36	45	—	1.50	1.760	1.0×10^{-9}	0.9
Dtc	1	44	25	55	30	17	1.70	1.50	1.195	2.6×10^{-9}	0.6
	2	48	25	61	36	30	1.19	1.50	1.297	9.8×10^{-10}	0.6
	3	40	24	58	33	32	1.04	1.50	1.070	4.6×10^{-10}	0.5
Ma12	1	79	38	104	65	35	1.86	1.40	2.101	1.2×10^{-9}	1.1
	2	55	29	76	47	39	1.19	1.40	1.453	5.4×10^{-10}	0.7
Doc1	1	47	22	71	48	29	1.67	1.40	1.260	4.6×10^{-10}	0.6
Ma11U	1	56	30	79	49	38	1.27	1.40	1.510	5.8×10^{-10}	0.8
	2	41	26	62	36	40	0.90	1.40	1.112	3.1×10^{-10}	0.6
Ma11L	1	49	28	70	42	29	1.44	1.40	1.328	8.2×10^{-10}	0.7
Ma10	1	43	30	72	42	30	1.40	1.50	1.171	4.5×10^{-10}	0.6
	2	56	35	92	57	23	2.54	1.50	1.499	8.0×10^{-10}	0.7
	3	64	37	102	65	27	2.43	1.50	1.731	8.1×10^{-10}	0.9
	4	48	32	84	52	29	1.82	1.50	1.292	4.2×10^{-10}	0.6
Ma9	1	55	35	91	57	28	2.04	1.30	1.480	6.1×10^{-10}	0.7
	2	51	34	90	56	39	1.45	1.30	1.383	3.0×10^{-10}	0.7
Doc5	1	63	39	105	66	36	1.85	1.35	1.645	4.4×10^{-10}	0.8
	2	52	36	84	47	52	0.92	1.35	1.378	2.4×10^{-10}	0.7
Ma8	1	44	31	83	51	33	1.55	1.30	1.174	2.4×10^{-10}	0.6
	2	54	36	91	56	33	1.67	1.30	1.448	4.6×10^{-10}	0.7
	3	46	32	60	28	33	0.84	1.30	1.241	1.1×10^{-9}	0.6
Ma7	1	48	33	80	46	28	1.64	1.28	1.280	5.6×10^{-10}	0.6
	2	54	37	96	59	29	2.05	1.28	1.460	4.9×10^{-10}	0.7
	3	46	33	83	50	45	1.12	1.28	1.231	1.8×10^{-10}	0.6
Doc6	1	46	34	89	54	36	1.49	1.28	1.243	2.3×10^{-10}	0.6
Ma4	1	49	34	87	53	30	1.75	1.30	1.303	3.8×10^{-10}	0.7
Ma3	1	50	35	86	50	29	1.76	1.35	1.348	5.5×10^{-10}	0.7
Ma2	1	41	31	82	51	28	1.83	1.35	1.096	2.4×10^{-10}	0.5
NMC-1	1	35	29	78	50	26	1.91	1.35	0.927	1.5×10^{-10}	0.5
NMC-2	1	29	23	57	34	30	1.13	1.35	0.774	1.3×10^{-10}	0.4
NMC-3	1	32	24	63	38	21	1.86	1.35	0.865	3.0×10^{-10}	0.4
Ma1	1	39	32	84	51	26	1.99	1.30	1.036	2.1×10^{-10}	0.5
NMC-4	1	25	18	35	16	6	2.58	1.30	0.659	4.6×10^{-9}	0.3
Ma0	1	32	25	63	38	14	2.67	1.40	0.861	4.8×10^{-10}	0.4
NMC-5	1	19	25	62	37	12	3.04	1.40	0.515	7.8×10^{-11}	0.3

Note: Natural water content, Atterberg limits, and clay-size fraction values are the average of all available data at the Kansai Airport site and are used to compute e_o and k_{vo} for settlement analyses at MP1-I and MP2-II.

[a]CF values for Ma13 represent percentage <5 μm.

The entire water content data for Ma13 and Ma10 are plotted in Fig. 3. The data are shown with respect to the depth into the layer (z) divided by the prereclamation layer thickness (L_o) so that comparisons can be made at various boreholes at the Kansai Airport site. This was a practical and convenient way to subdivide the marine clay layers at the airport site, especially because the distance between boreholes (e.g., maximum distance of approximately 8.5 km) across the site is relatively small for a marine depositional environment. A plot of available data similar to Fig. 3 was prepared for all the 21 Pleistocene clay layers from Dtc to NMC-5 listed in Table 1.

Permeability of Osaka Bay Sediments

The literature on Kansai Airport does not appear to include any permeability data from direct permeability tests on Osaka Bay clay or sand layers.

For the present settlement analyses, the values of k_{vo} for the Pleistocene clay layers were computed using the Mesri et al. (1994) equation together with representative values of prereclamation void ratio (e_o), clay-size fraction (CF), and activity ($A_c = I_p/\text{CF}$) in Table 1. Rocchi et al. (2006) compared permeability data for Osaka Bay clays with k_{vo} computed using the Mesri et al. (1994) equation, concluding that the empirical relationship provides a good fit to the experimental data for Osaka clays. The values of k_{vo} for Pleistocene clays computed using the Mesri et al. (1994) equation are listed in Table 1.

The values of k_{vo} for Ma13 clay sublayers, in the absence of reliable data on CF, were based on permeability data determined by Tanaka et al. (2003) by interpreting, using the Terzaghi theory of consolidation, compression rates observed in incremental loading oedometer tests. However, Mesri et al. (1994) showed that the values of permeability computed from c_v and m_v typically underestimate k_v

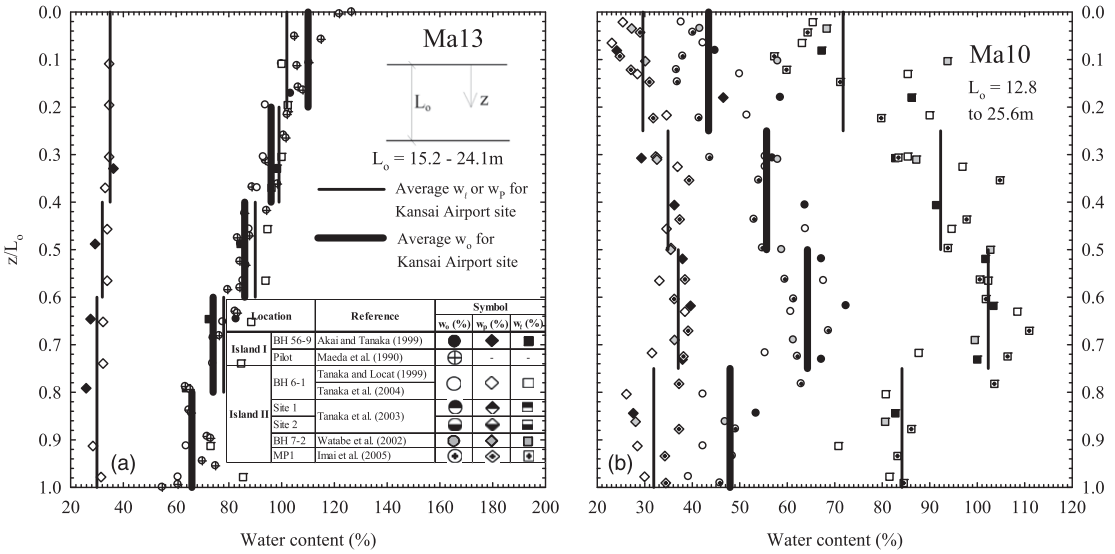

Fig. 3. Atterberg limits and natural water content for (a) Ma13; (b) Ma10

by a factor of 2. Therefore, the values of k_{vo} for Ma13 in Table 1 were obtained by increasing the Tanaka et al. (2003) data by a factor of 2.

Permeability is expected to decrease with the decrease in void ratio, and for clays, the e-log k_v, with slope $C_k = \Delta e/\Delta \log k$, is commonly used (Tavenas et al. 1983; Mesri et al. 1994). The value of C_k for each sublayer listed in Table 1 was computed using $C_k = 0.5e_o$ proposed by Tavenas et al. (1983) and confirmed by Mesri et al. (1994). Tanaka et al. (2003) showed that $C_k = 0.5e_o$ is also applicable to Osaka Bay clays.

The sand layers in Osaka Bay play a significant role on the rate of consolidation of the clay layers and therefore on rate of settlement of the airport islands. Nakase (1987) listed the range of permeabilities for Pleistocene sand layers as 10^{-8} to 10^{-5} m/s. Mimura and Jang (2005) attributed the existence of undissipated pore-water pressures to low permeability and discontinuity of sand layers, considering the permeability question unresolved. For a settlement analysis of Island I, Mimura and Jang (2005) assumed Ds10 to be freely draining, Ds1 to have a high permeability of 10^{-2} m/s, and assigned permeability values in the range of 2.5×10^{-7} to 4.5×10^{-5} m/s to the remaining sand layers. In settlement analyses of Kansai Airport Islands, Shibata and Karube (2005) assumed permeability values in the range of 1×10^{-5} to 8.5×10^{-5} m/s for the sand layers. Kobayashi et al. (2005), in terms of thickness and continuity, considered Ds1 and Ds10 to function as drainage layers.

The permeability of the Pleistocene sand layers was back-calculated for the present settlement analyses of Islands I and II using observed settlements and pore-water pressures. The same *ILLICON* procedure (Funk and Mesri 2014) to be described later, which was used for the long-term settlement analyses of the Pleistocene clay layers, was used for the back-analyses. In both back-analyses, to compute the permeability of the sand layers and long-term settlement analyses, one-dimensional vertical compression in clay layers and vertical and horizontal water flow in the clay layers were assumed. Horizontal flow in the sand layers was assumed. The horizontal drainage boundary is set at points where $\Delta\sigma_v$ from reclamation load and therefore u_o' is small (influence factor for the vertical stress increase using the Boussinesq solution is less than 0.001). Sand layers Ds1 and Ds10 were assumed to be freely draining, and the back-analyses resulted in permeability of the remaining sand layers in the range of 10^{-7} to 10^{-4} m/s (Funk 2013), comparable to the range of values reported by Nakase (1987), Mimura and Jang (2005), and Shibata and Karube (2005).

Compressibility of Osaka Bay Clay Layers

The *ILLICON* procedure used here for settlement analyses of the Kansai International Airport Islands is based on the assumption of uniqueness of the EOP void ratio–effective vertical stress relationship and the C_α/C_c law of compressibility. For each sublayer, such as those in Table 1, an EOP e-log σ_v' relationship and a single value of C_α/C_c are required for settlement analysis. All published incremental loading and constant rate of deformation oedometer test data were used to define compressibility of the clay layers at the Kansai Airport site (Kanda et al. 1991; Tanaka et al. 2003, 2004; Tanaka 2005a, b; Furudoi and Kobayashi 2009). For the Pleistocene clay samples from depths below the seafloor range of 60–400 m, the values of ε_{vo}, according to oedometer compression data, are in the range of 1.8–4.0%, suggesting a specimen quality designation of B to C (Terzaghi et al. 1996).

Published data on e_o, σ_{vo}', C_r/C_c, σ_p'/σ_{vo}', and the nonlinear e-log σ_v' relationship in the compression range beyond σ_p' were used to construct for each sublayer the EOP e-log σ_v' relationship, which was input into the *ILLICON* computer program. The EOP e-log σ_v' relationship of all clay layers starts at (e_o, σ_{vo}') in the recompression range. The representative values of e_o in Table 1 were calculated from published w_o data (Maeda et al. 1990; Akai and Tanaka 1999; Tanaka and Locat 1999; Tanaka et al. 2003, 2004; Imai et al. 2005) and G_s data (Akai and Tanaka 1999). Prereclamation hydrostatic pore-water pressure from sea level was used to compute σ_{vo}' and to interpret postreclamation pore-water pressure measurements. The values of σ_{vo}' at MP2-II are shown in Fig. 4. The published total unit weight data for the clay and sand layers were used to calculate σ_{vo} and therefore σ_{vo}'.

The values of σ_p'/σ_{vo}' for the clay layers at the Kansai Airport site were obtained from incremental loading (IL) and constant rate of strain (CRS) oedometer tests on undisturbed specimens. The value of σ_p' for IL tests was obtained using the EOP e-log σ_v' relationship. It is well established that the value of σ_p' from CRS tests is a function of the imposed strain rate. Mesri and Feng (1986) recommended the EOP strain rate $\dot{\varepsilon}_p$ to obtain the EOP e-log σ_v' relationship from the CRS oedometer tests. For typical soft clay deposits, the value of $\dot{\varepsilon}_p$ is

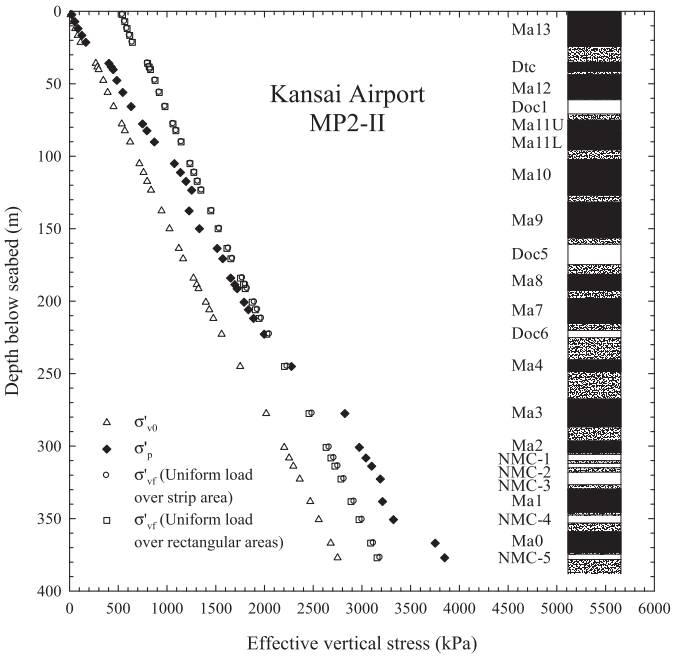

Fig. 4. Vertical profile of preconstruction effective vertical stress (σ'_{vo}), preconsolidation pressure (σ'_p), and maximum final effective vertical stress (σ'_{vf}) at MP2-II

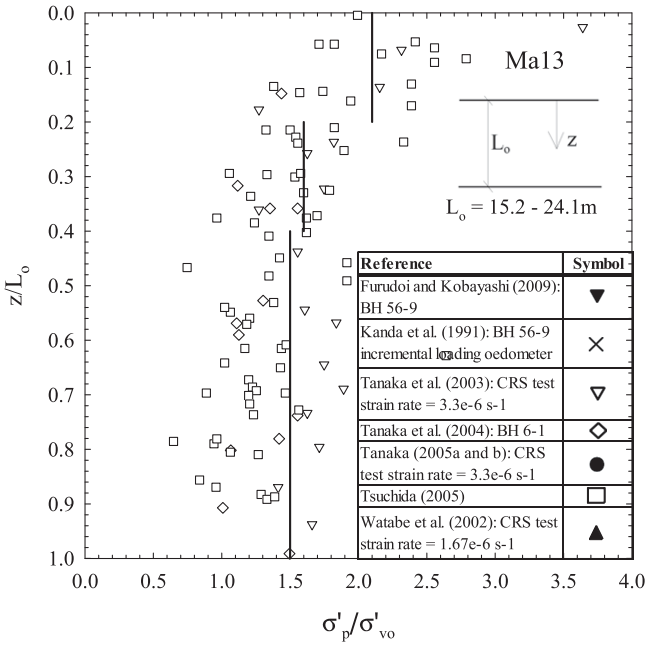

Fig. 5. σ'_p/σ'_{vo} for Ma13

$2.7 \times 10^{-7}\ s^{-1}$ (Mesri et al. 1994). The σ'_p/σ'_{vo} data for Osaka Bay clays include CRS tests with $\dot{\varepsilon}_I = 3.3 \times 10^{-6}\ s^{-1}$ (Tanaka et al. 2003; Tanaka 2005a, b) and $\dot{\varepsilon}_I = 1.6 \times 10^{-6}\ s^{-1}$ (Watabe et al. 2002). Therefore, the reported values of σ'_p/σ'_{vo} were reduced by a factor of 0.90 and 0.93, respectively, according to the empirical equation by Mesri and Feng (1986).

The values of σ'_p/σ'_{vo} for Holocene Clay Layer Ma13 are shown in Fig. 5 together with vertical line segments indicating the values that were used in the *ILLICON* settlement analyses. Similar plots were prepared for all Pleistocene clay layers, with four examples shown in Fig. 6. In Pleistocene clay layers, the values of σ'_p/σ'_{vo} used for *ILLICON* analyses, listed in Table 1, ranged from 1.28 to 1.50. The preconsolidation pressure of Osaka Bay clays has mainly resulted from aging including secondary compression and thixotropic hardening and, possibly, some carbonate cementation (Mesri and Choi 1979; Tsuchida 2005).

The compression of Osaka Bay clays beyond the preconsolidation pressure, from IL and CRS oedometer tests, was summarized in terms of the secant compression index C'_c versus $\log \sigma'_v/\sigma'_p$, where σ'_v is the effective vertical stress for which C'_c is defined (Mesri and Choi 1985a; Terzaghi et al. 1996, Fig. 16.6). The C'_c-$\log \sigma'_v/\sigma'_p$ plot for Holocene Marine Clay Layer Ma13 and the Pleistocene clays are shown in Figs. 7 and 8, respectively.

The EOP e-$\log \sigma'_v$ relationship for each sublayer listed in Table 1 was constructed (Funk 2013) starting from point (e_o, σ'_{vo}) with a recompression curve defined by $C_r/C_c = 0.1$, where C_c is the compression index from σ'_p to $2\sigma'_p$, up to σ'_p, and then defining the nonlinear compression curve using four to six values of (C'_c, σ'_v/σ'_p).

The secondary compression of Osaka Bay clays following primary consolidation was defined using the C_α/C_c law of compressibility, which requires for each sublayer the EOP e-$\log \sigma'_v$ relationship together with C_α/C_c, where at any consolidation pressure σ'_v, C_c is a tangent compression index (Mesri and Godlewski 1977; Mesri and Castro 1987; Mesri 2001; Mesri and Ajlouni 2007). The values of C_α/C_c for Osaka Bay clays were determined from the published IL oedometer test data (Imai et al. 2005; Tanaka 2005a, b; Watabe et al. 2008; Funk 2013). A special procedure was also used to compute C_α/C_c for 11 Pleistocene clay layers using long-term incremental loading compression data by Tanaka (2005a, b). For each Pleistocene clay specimen, the EOP e-$\log \sigma'_v$ curve and e-$\log t$ curves for two pressures in the recompression range were available. As is predicted by the C_α/C_c law of compressibility, the e-$\log t$ curve for the pressure near the preconsolidation pressure started with a small C_α proportional to the recompression index, rapidly increased to a maximum proportional to the maximum C_c on the EOP e-$\log \sigma'_v$ curve, and gradually decreased with time in accordance with the decrease in C_c in the compression range. Therefore, the maximum C_α was used together with the maximum C_c to define C_α/C_c. The values of C_α/C_c for 11 clay layers from Dtc to Ma2 were in the range of 0.024–0.042, with an average value of 0.033, which is quite similar to the value from the published IL oedometer test data. The resulting value of C_α/C_c for each clay layer together with the EOP e-$\log \sigma'_v$ curve were used to construct e-$\log \sigma'_v$ curves for $t/t_p > 1$. Four examples for the laboratory specimens are shown in Fig. 9, which also includes secondary compression measurements by Tanaka (2005b) at two consolidation pressures in the recompression range.

For reclamation loading in Osaka Bay, secondary settlement is expected to be a significant factor only for clay layers with a short duration of primary consolidation (t_p). This is only true for Holocene Marine Clay Layer Ma13 because of the use of vertical drains and for Pleistocene clay layers at great depth, e.g., Ma3 and lower in Fig. 2, where σ'_v is in the recompression range (Fig. 4) and therefore t_p is small.

Settlement Analyses for the Kansai Airport Islands

The *ILLICON* computer program was rebuilt especially to accommodate the sand layers at Osaka Bay as incompressible impeded drainage boundaries that discharge water in the horizontal direction. Detailed reclamation load history and settlement observations for the Holocene clay layer (Ma13) were available at Monitoring Point 1 of Island II (MP1-II), Monitoring Point 2 of Island II (MP2-II), the

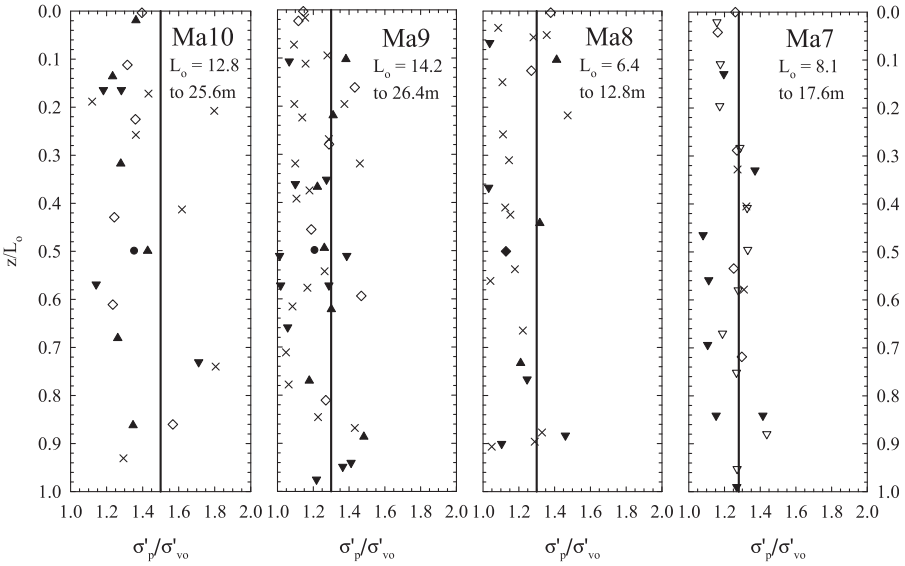

Fig. 6. σ'_p/σ'_{vo} for Pleistocene marine clay layers Ma10, Ma9, Ma8, and Ma7 (symbols defined in Fig. 5)

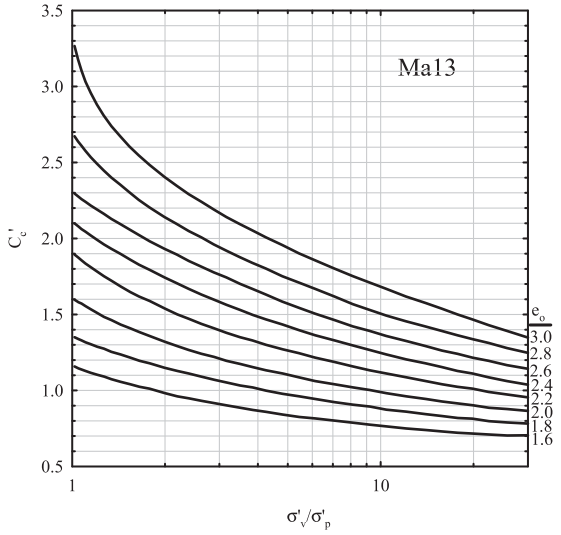

Fig. 7. C'_c for Ma13

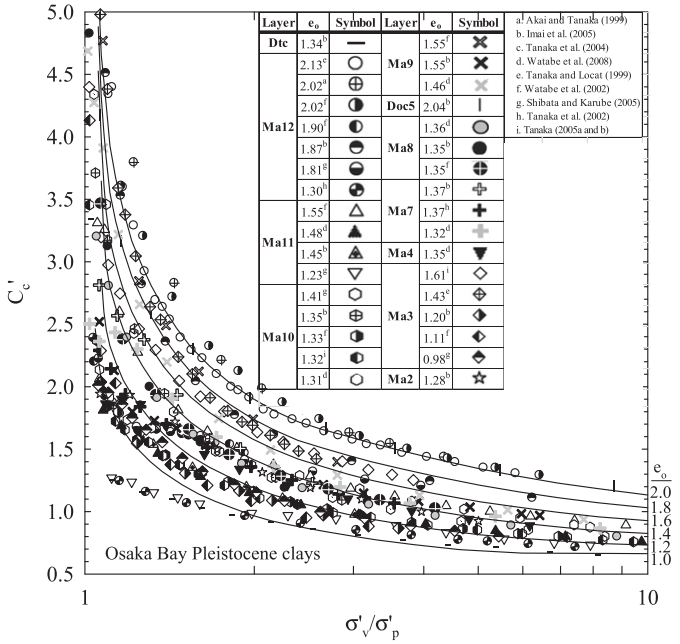

Fig. 8. C'_c for Pleistocene clay layers

Connecting Taxiway (CT), Point K of Island I (K-I), and Monitoring Point 1 of Island I (MP1-I). Therefore, settlement analyses of the Ma13 clay layer were carried out at these locations. Detailed settlement and pore-water pressure observations for the Pleistocene clay layers were available at MP1-II, MP2-II, and MP1-I, and settlement analyses at these locations were carried out to include clay layers to a depth of up to 400 m below the seafloor.

ILLICON Computer Program

The *ILLICON* computer program was rebuilt using Microsoft Visual Studio 2010 (Redmond, Washington) to facilitate settlement and pore-water pressure calculation for the Kansai International Airport. A user interface that provides graphical output was created as a Windows Form Application, and the computational core was coded using Microsoft Visual C++. The current version of *ILLICON*, which is based on the Darcy flow equation, uniqueness of EOP e-log σ'_v relationship, and the C_α/C_c law of compressibility, retains all features listed in Mesri and Khan (2012).

The hydrodynamic equation used for the Holocene Ma13 clay layer with vertical water flow into the sand blanket overlying Ma13, as well as the sand layer Ds1 underlying Ma13 and radial water flow into the vertical drain is

$$\frac{de}{dt} = \frac{1}{\gamma_w}\left(\frac{1+e_o}{1+e}\right)^2\left[(1+e)\left(k_z\frac{\partial^2 u'}{\partial z^2}+\frac{\partial k_z}{\partial z}\frac{\partial u'}{\partial z}\right)-k_z\frac{\partial u'}{\partial z}\frac{\partial e}{\partial z}\right] + \frac{1+e}{\gamma_w}\left[k_r\left(\frac{1}{r}\frac{\partial u'}{\partial r}+\frac{\partial^2 u'}{\partial r^2}\right)+\frac{\partial k_r}{\partial r}\frac{\partial u'}{\partial r}\right] \quad (1)$$

The hydrodynamic equation used for the Pleistocene clay layers with vertical water flow into sand layers that are treated as impeded

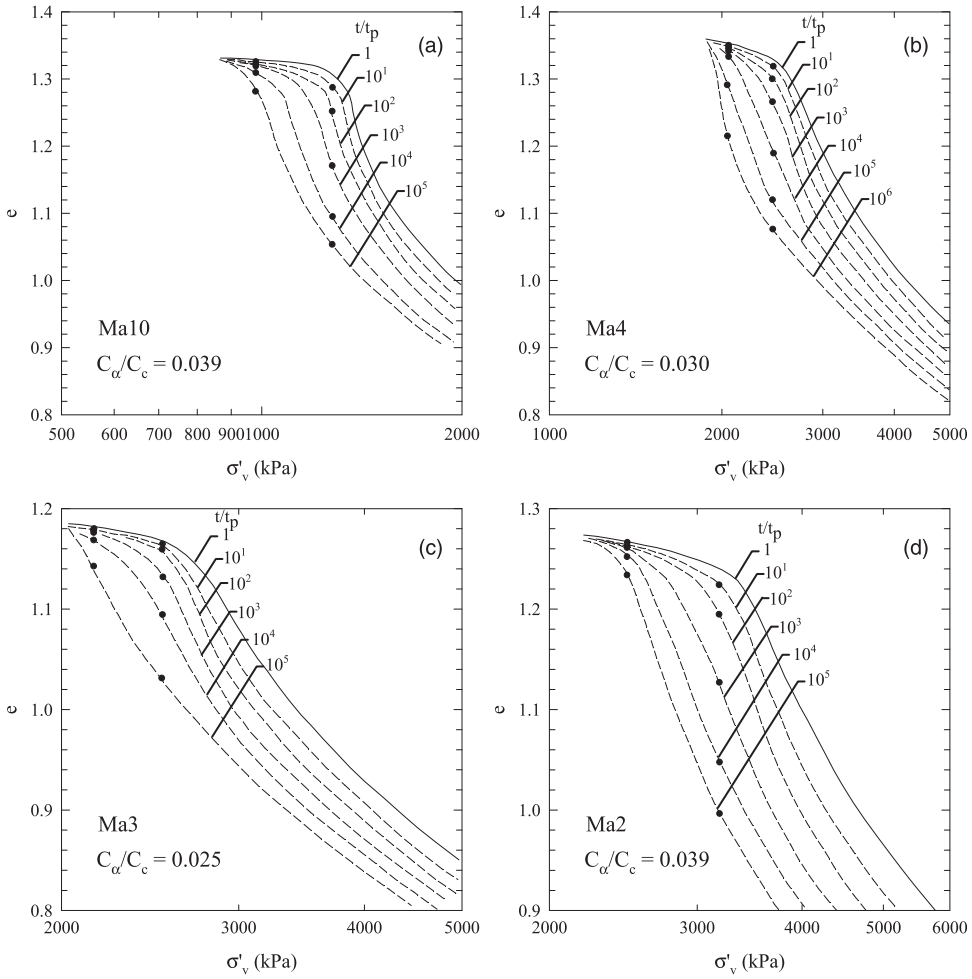

Fig. 9. e-log σ_v' curves for $t/t_p > 1$ for Pleistocene clay layer (a) Ma10, (b) Ma4, (c) Ma3, and (d) Ma2, constructed using the EOP e-log σ_v' curve together with C_α/C_c; the data points are from the long-term IL compression measurements by Tanaka (2005b)

drainage boundaries and horizontal water flow within the consolidating clay layer is (Funk 2013)

$$\frac{de}{dt} = \frac{1}{\gamma_w}\left(\frac{1+e_o}{1+e}\right)^2\left[(1+e)\left(k_z\frac{\partial^2 u'}{\partial z^2}+\frac{\partial k_z}{\partial z}\frac{\partial u'}{\partial z}\right)-k_z\frac{\partial u'}{\partial z}\frac{\partial e}{\partial z}\right] + \frac{1+e}{\gamma_w}\left[k_x\frac{\partial^2 u'}{\partial x^2}+\frac{\partial k_x}{\partial x}\frac{\partial u'}{\partial x}\right] \tag{2}$$

Because the length to width ratio of Kansai Airport Island I and Kansai Airport Island II is more than 3.5, the hydrodynamic equation for the Pleistocene clay layers was developed assuming vertical water flow plus horizontal water flow perpendicular to the length of each Airport Island (i.e., the x-direction).

The constitutive equation used in the *ILLICON* approach is (Mesri 2001)

$$\frac{\partial e}{\partial t} = \left(\frac{\partial e}{\partial \sigma_v'}\right)_t \frac{\partial \sigma_v'}{\partial t} + \left(\frac{\partial e}{\partial t}\right)_{\sigma_v'} \tag{3}$$

The compressibility parameters $(\partial e/\partial \sigma_v')_t$ and $(\partial e/\partial t)_{\sigma_v'}$ are evaluated assuming the uniqueness of the EOP e-σ_v' relationship together with the C_α/C_c law of compressibility (Funk 2013). The explicit finite-difference approximation was used to solve the hydrodynamic and constitutive equations together (Funk 2013).

The compression of the Holocene Ma13 clay layer observed at CT, K-I, and MP1-I, together with *ILLICON* predictions, is shown in Figs. 10(a–c), respectively [for MP1-II and MP2-II, see Funk (2013)]. The settlements of the Pleistocene clay layers observed at MP1-II, together with *ILLICON* predictions, are shown in Fig. 11. The excess pore-water pressure observations in the Pleistocene sand layers at MP1-II, together with *ILLICON* predictions, are shown in Fig. 12. The settlements of Pleistocene clay layers observed at MP1-I, together with *ILLICON* predictions, are shown in Fig. 13. The excess pore-water pressure observations in the Pleistocene sand layers, together with *ILLICON* predictions, are shown in Fig. 14. The pore-water pressure increases in the Pleistocene sand layers through redistribution from the reclamation of Airport Island II. This pore-water pressure redistribution is expected to somewhat slow down settlement of Airport Island I, as suggested by the open and solid circles in Fig. 13.

Interpretations of Field Observations Together with *ILLICON* Predictions

Large settlements of the Kansai International Airport islands have resulted from the large total thickness of Holocene plus Pleistocene

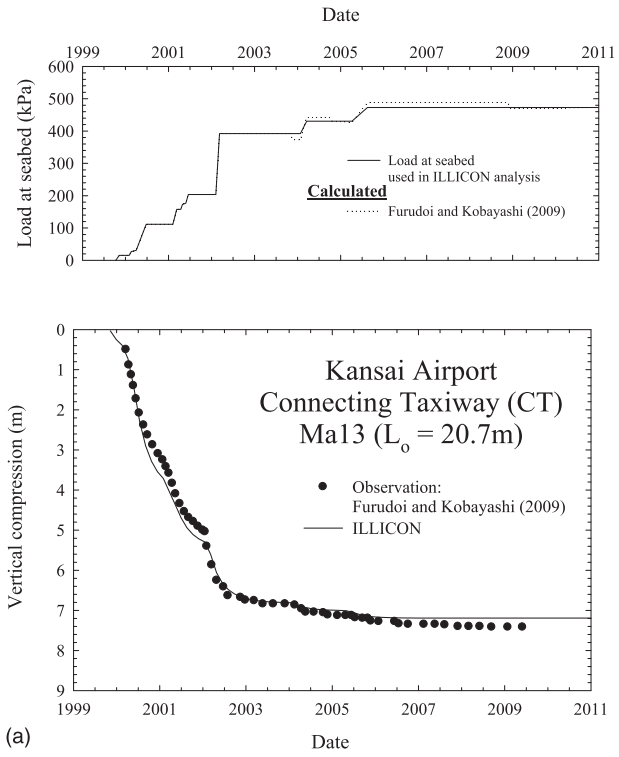

Fig. 10. (a) Load at seabed used in analysis together with observed and computed vertical compression of Ma13 at CT; (b) load at seabed used in analysis together with observed and computed excess pore-water pressure and vertical compression of Ma13 at K-I; (c) load at seabed used in analysis together with observed and computed vertical compression of Ma13 at MP1-I

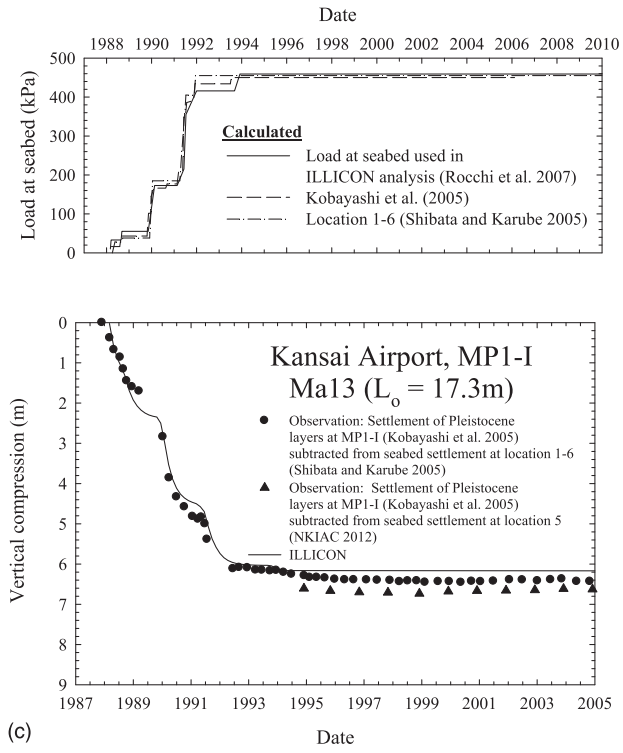

Fig. 10. (*Continued*.)

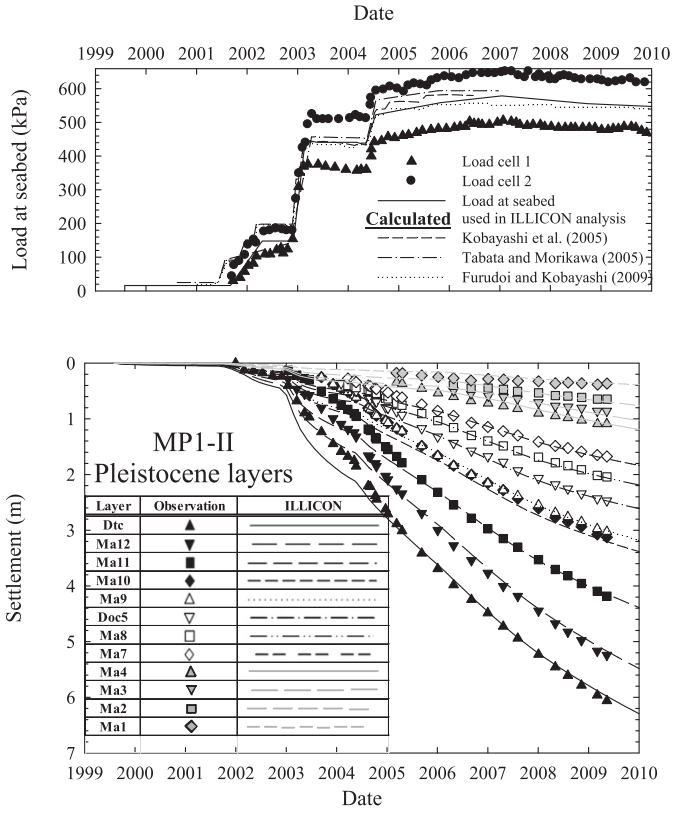

Fig. 11. Observed (data from Furudoi and Kobayashi 2009) and calculated settlement of Pleistocene layers at MP1-II to the year 2010

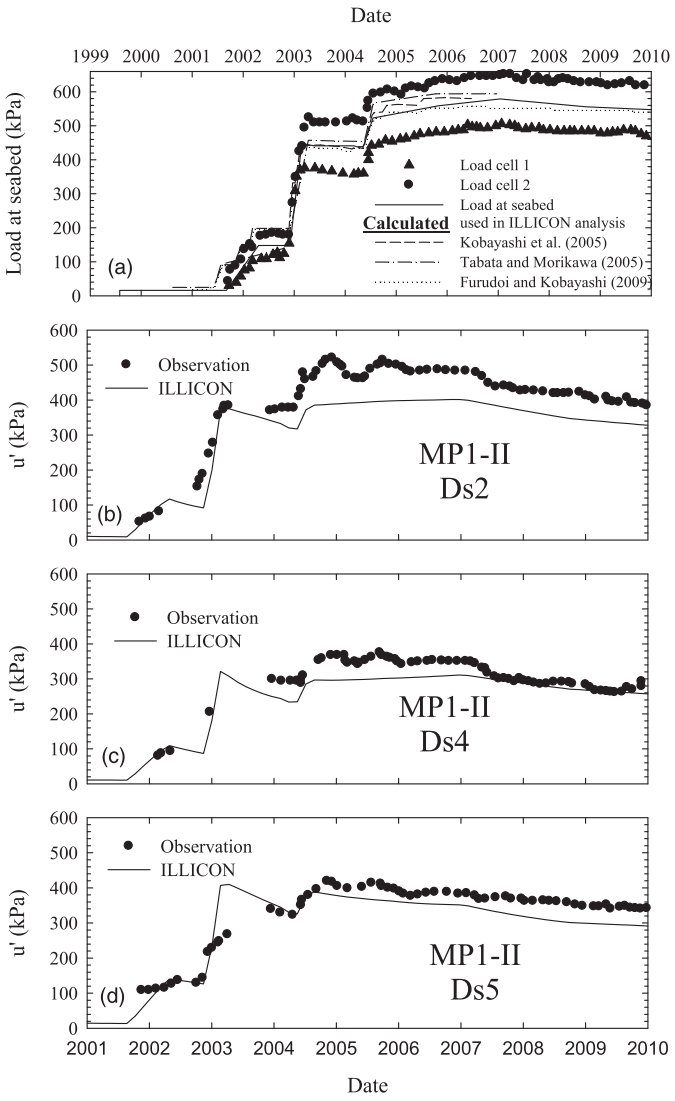

Fig. 12. Observed (data from Furudoi 2010) and calculated excess pore-water pressures at MP1-II

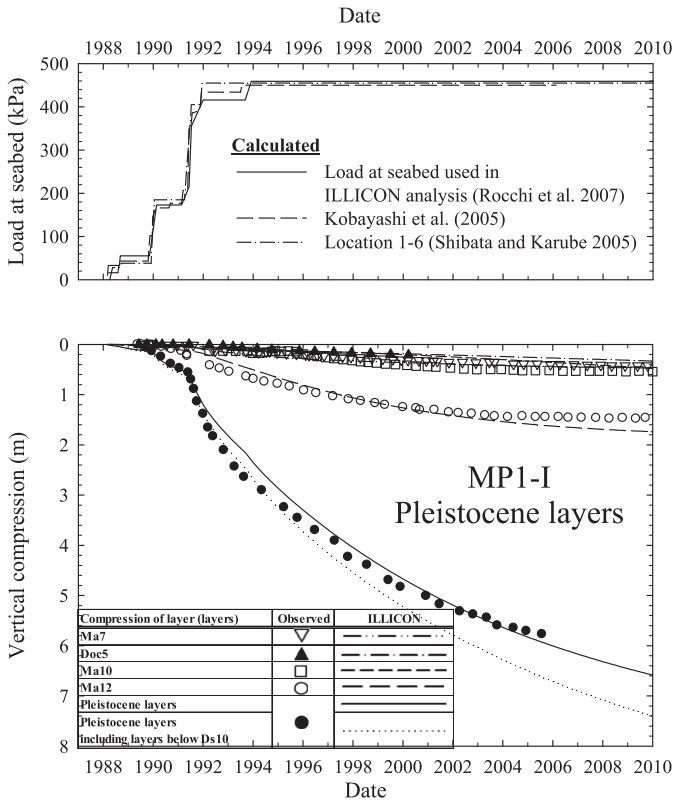

Fig. 13. Observed (data from Kobayashi et al. 2005; Rocchi et al. 2007; Jeon et al. 2012) and calculated compression of Pleistocene layers at MP1-I to the year 2010

clay layers and large reclamation loads. According to the *ILLICON* analyses shown in Fig. 15 and Table 2, by the end of the 21st century, MP1-II on Airport Island II will settle 24.4 m. Table 2 shows that at MP1-II a combined 185.3 m thickness of clay (Ma13 to Doc6) was loaded to the compression range with maximum σ'_{vf}/σ'_p in the range of 1.05–2.15, and a combined 102.0-m thickness of Pleistocene clay (Ma4 to NMC-5) was loaded to the recompression range with maximum σ'_{vf}/σ'_p in the range of 0.83–1.01. The clay layers Ma13 to Doc6 contribute significant primary settlement, whereas Ma4 to NMC-5 because of short duration of primary consolidation (t_p) in the recompression range (together with rapid increase in C_α with time near σ'_p) and Ma13 with small t_p because of vertical sand drains contribute significant secondary settlement. A similar behavior is displayed in Fig. 16 for MP2-II and in Fig. 17 and Table 3 for MP1-I.

The comparison of observations of settlement and pore-water pressure with those predicted by the *ILLICON* analyses suggest that the phenomenon taking place at Osaka Bay because of the airport reclamation can be explained according to conventional concepts of primary compression followed by secondary compression (Mesri and Godlewski 1977, 1979; Mesri and Choi 1985a, b; Mesri et al. 1994; Mesri 2001). The observed in situ strain and thus settlement are similar to values predicted by *ILLICON* analyses almost entirely based on input data from laboratory tests. According to the C_α/C_c law of compressibility, clay layers subjected to values of σ'_{vf}/σ'_p in the range of 0.75–1.0 are expected to rapidly complete primary consolidation and then display secondary compression, initially without showing a tendency of decreasing coefficient of secondary compression such as shown in Fig. 9.

The behavior of Holocene and Pleistocene clay layers at the Kansai International Airport site is not different in any fundamental way from the experience that has been available for clays from throughout the world. The total thickness of clay layers, the magnitude of reclamation loads, and impeded drainage boundary conditions provided by the Pleistocene sand layers combine together to lead to large time-dependent settlement of the airport. According to Fig. 17, Airport Island I exceeded the design requirement of 4 m above sea level in 2001 and will be at sea level by 2067 or possibly much sooner. Airport Island II, according to Figs. 15 and 16, will be at the design requirement of 4 m above sea level by 2023–2036 and will be at sea level by 2058–2100.

Summary and Conclusions

The following summary and conclusions are based on the data, analyses, and interpretation presented in this paper:

1. The basement rock, located at depths greater than 1,000 m at the Kansai Airport site, is overlain by freshwater deposits followed by an alternating sequence of Pleistocene marine and

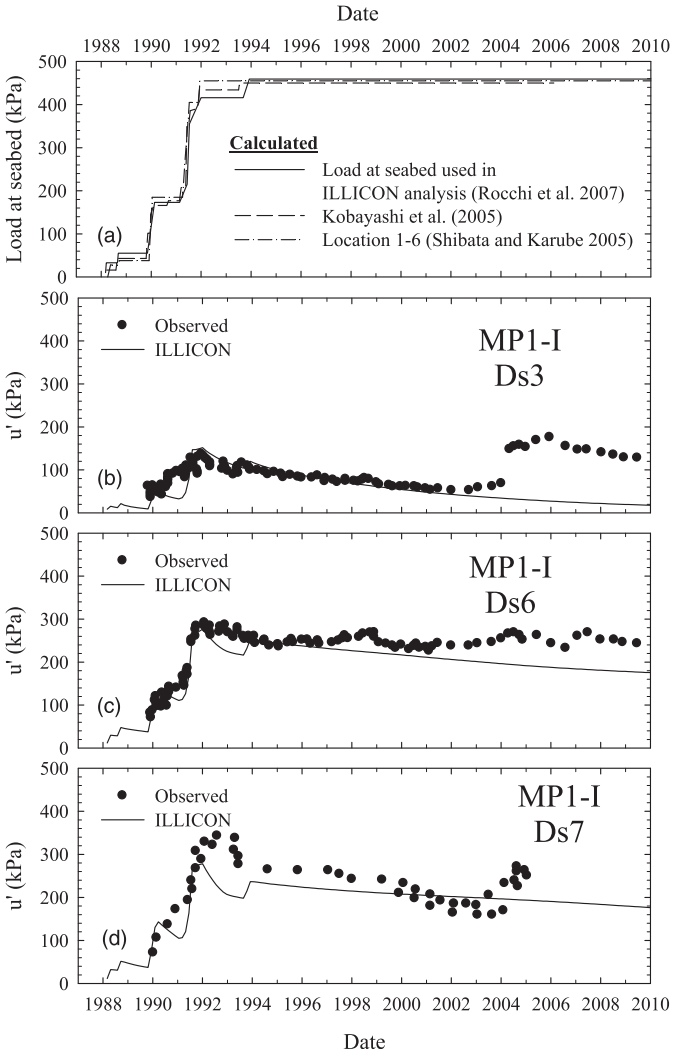

Fig. 14. Observed (data from Kobayashi et al. 2005; Jeon et al. 2012) and calculated excess pore-water pressures at MP1-I

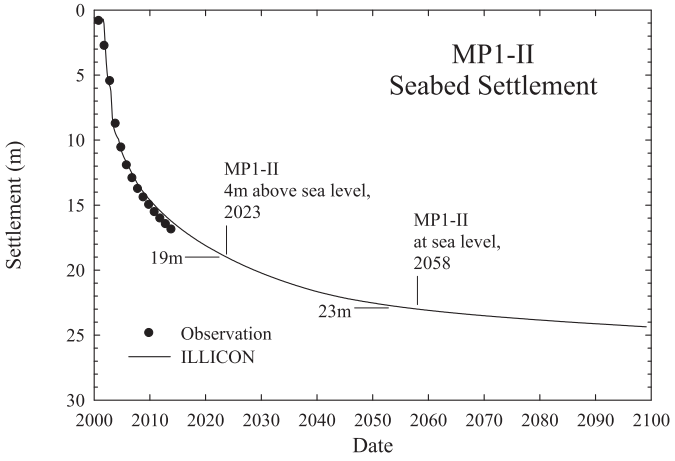

Fig. 15. Seabed settlement at MP1-II, including compression of Holocene and Pleistocene clay layers

nonmarine clay and sand layers. The Pleistocene marine and nonmarine clay and sand deposits together with an overlying 17- to 25-m-thick Holocene marine clay layer constitute the upper 400 m of the subseabed profile at the airport site. The upper 400 m of the subseabed profile at Monitoring Point 1 of Airport Island II (MP1-II) consists of 22 clay layers with a combined total thickness of 290 m and 19 sand layers with a combined total thickness of 110 m. The lowermost Pleistocene clay layer was deposited 1 million YBP, and deposition of the Holocene clay layer began 10,000–12,000 YBP.

2. The prereclamation subseabed condition at the Kansai Airport site was defined by 63 borings made to depths of 100–200 m below seabed and six borings made to a depth of 400 m below the seabed. Representative values of natural water content, plastic limit, liquid limit, clay-size fraction, and activity for 22 clay layers are in the range of 19 (lowermost Pleistocene nonmarine clay layer NMC-5) to 110% (uppermost sublayer of Holocene marine clay layer Ma13), 18–41%, 35–110%, 6–52%, and 0.99 to 3.04, respectively.
3. For the *ILLICON* settlement analyses, in the absence of reported direct measurements of permeability, vertical permeability (k_{vo}) of the Pleistocene clay layers in the range of 7.8×10^{-11} to 4.6×10^{-9} m/s was calculated using the empirical equation by Mesri et al. (1994) together with representative values of prereclamation void ratio, clay-size fraction, and activity for each sublayer. Vertical permeability values for the Holocene clay sublayers, in the range of 1.0×10^{-9} to 2.3×10^{-8} m/s, were determined based on compression rates in incremental loading oedometer tests interpreted using the Terzaghi theory of consolidation. For all clay layers, the decrease in permeability during consolidation was calculated using the empirical equation $C_k = 0.5e_o$.
4. In the absence of reported direct measurements, values of $k_v = k_h$ for the Pleistocene sand layers were back-calculated using the *ILLICON* computer program together with settlement and pore-water pressure observations, assuming one-directional horizontal flow within the sand layers that is perpendicular to the long dimension of each airport island. The back-calculated permeability values were in the range of 10^{-7} to 10^{-4} m/s, which is comparable to values used in settlement analyses performed by others in the literature for the Kansai Airport islands.
5. The compressibility of each clay sublayer was defined in terms of an EOP e-log σ'_v relationship together with a single value of C_α/C_c. The EOP e-log σ'_v relationship of each sublayer started from the prereclamation point (e_o, σ'_{vo}) continued along a recompression curve assuming $C_r/C_c = 0.1$ to a preconsolidation pressure computed from σ'_p/σ'_{vo} data in the range of 1.28–2.10 for Holocene and Pleistocene clay layers and then to a nonlinear compression curve constructed using C'_c-log σ'_v/σ'_p data from all published IL and CRS oedometer tests on Holocene and Pleistocene clays from the Kansai Airport site.
6. Computed EOP compression of Ma13 is 5.8 m at MP1-I, 8.1 m at MP2-II, and 8.3 m at MP1-II. According to observations and *ILLICON* analyses, primary consolidation of the Holocene Ma13 clay layer was realized soon after reclamation was completed in each location because of the presence of vertical drains. As of December 2012, the average observed seabed settlement has exceeded 12.9 and 14.2 m, respectively, for Airport Islands I and II.
7. According to the *ILLICON* analyses, by the end of the 21st century, MP1-I on Island I will settle 17.6 m and MP1-II and MP2-II on Island II will settle 24.4 and 22.9 m, respectively.

Table 2. Summary of Calculations for Compression of Pleistocene Clay Layers at MP1-II

Layer	L_o (m)	t_p from July 1999 (years)	Date when t_p reached	σ'_{vf}/σ'_p (Jan. 2007)	EOP compression (m)[a]	Primary compression in 2100 (m)	Secondary compression in 2100 (m)
Ma13	24.1	5.1	Sep. 2004	4.13–25.34	8.25	8.25	0.30
Dtc	7.6	67.8	May 2067	1.97–2.15	0.92	0.92	0.01
Ma12	15.1	67.8	May 2067	1.79–1.91	2.40	2.40	0.11
Doc1	9.5	67.8	May 2067	1.63	1.16	1.16	0.05
Ma11U	10.8	43.5	Feb. 2043	1.44–1.49	1.18	1.18	0.05
Ma11L	9.8	β_{avg} = 92% in year 2100		1.36	1.15	0.91	—
Ma10	25.6	β_{avg} = 57% in year 2100		1.12–1.20	1.92	0.81	—
Ma9	26.4	β_{avg} = 90% in year 2100		1.19–1.23	2.35	1.74	—
Doc5	15.5	β_{avg} = 91% in year 2100		1.09–1.11	0.95	0.63	—
Ma8	12.8	80.8	May 2080	1.09–1.10	0.49	0.49	0.05
Ma7	17.6	92.8	Jun. 2092	1.07–1.09	0.53	0.53	0.03
Doc6	10.5	22.2	Oct. 2021	1.05	0.29	0.29	0.23
Ma4	8.1	5.5	Jan. 2005	1.01	0.05	0.05	0.39
Ma3	21.3	7.5	Feb. 2007	0.92	0.13	0.13	0.98
Ma2	10.4	7.3	Nov. 2006	0.93	0.05	0.05	0.43
NMC-1	5.1	6.3	Nov. 2005	0.92	0.02	0.02	0.20
NMC-2	4.2	6.2	Oct. 2005	0.91	0.02	0.02	0.18
NMC-3	10.7	6.4	Jan. 2006	0.90	0.05	0.05	0.43
Ma1	10.8	6.4	Jan. 2006	0.92	0.04	0.04	0.42
NMC-4	15.4	6.4	Jan. 2006	0.92	0.07	0.07	0.69
Ma0	13.6	6.0	Aug. 2005	0.83	0.05	0.05	0.04
NMC-5	2.4	5.1	Sep. 2004	0.83	0.01	0.01	0.00
				$\sum$	22.06	19.78	4.60

Note: EOP compression calculated from EOP void ratio for Ma11L through Doc5.

[a]EOP compression corresponds to β_{avg} = 95% for Ma13 through Ma11U and Ma8 through NMC-5.

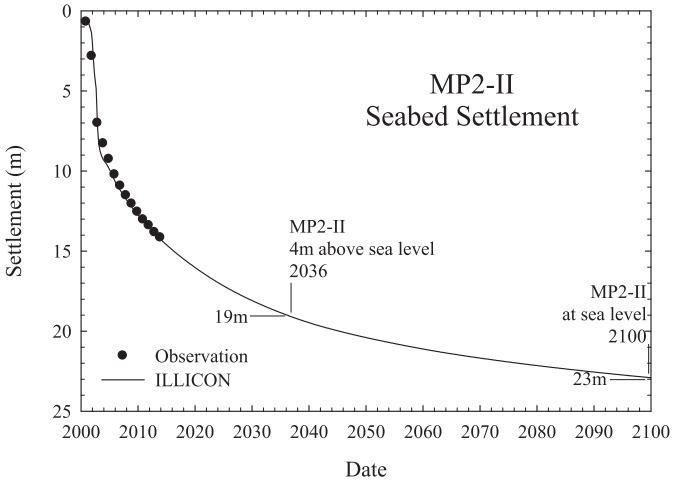

Fig. 16. Seabed settlement at MP2-II, including compression of Holocene and Pleistocene clay layers

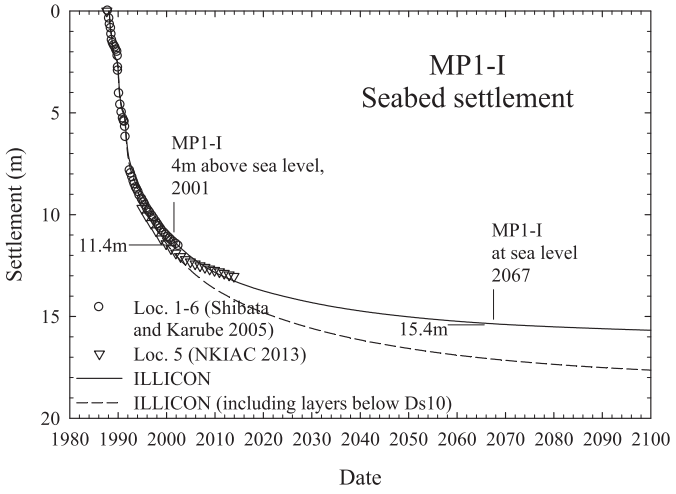

Fig. 17. Seabed settlement at MP1-I, including compression of Holocene and Pleistocene clay layers

8. At MP1-II, 185.3-m combined thickness of clay (Ma13 to Doc6) was loaded to the compression range with maximum σ'_{vf}/σ'_p in the range of 1.05–2.15 and has experienced significant primary compression. On the other hand, 102.0-m combined thickness of Pleistocene clay (Ma4 to NMC-5) was loaded to the recompression range with maximum σ'_{vf}/σ'_p in the range of 0.83–1.01, and because of the short duration of primary consolidation together with rapid increase in C_α with time, is expected to experience significant secondary compression.
9. In 2001, Airport Island I exceeded the design specification requiring that the surface elevation of the airport islands should remain 4 m above sea level. By 2067 or sooner, Island I is predicted to be at sea level. The surface elevation of Airport Island II is predicted to be at the design requirement of 4 m above sea level by 2023–2036, and Airport Island II is predicted to be at sea level by 2058–2100.
10. According to the *ILLICON* predictions, 100 years after construction of Airport Island II, the degree of primary compression of the 24.5- to 25.6-m-thick Ma10 Pleistocene clay layer with impeded drainage boundaries will be 54–57%.

Table 3. Summary of Calculations for Compression of Pleistocene Clay Layers at MP1-I

Layer	L_o (m)	t_p from Jan. 1987 (years)	Date when t_p reached	σ'_{vf}/σ'_p (Sep. 1991)	EOP compression (m)[a]	Primary compression in 2100 (m)	Secondary compression in 2100 (m)
Ma13	17.3	7.5	Jun. 1994	4.31–24.71	5.79	5.79	0.56
Dtc	4.0	23.6	Aug. 2010	1.97–2.09	0.46	0.46	0.03
Ma12	9.8	23.6	Aug. 2010	1.90–2.03	1.75	1.75	0.16
Doc1	2.2	23.6	Aug. 2010	1.82	0.35	0.35	0.02
Ma11U	6.9	29.4	May. 2016	1.57–1.62	0.95	0.95	0.07
Ma11L	6.0	61.3	Apr. 2048	1.47	0.73	0.73	0.04
Ma10	15.4	92.1	Jan. 2079	1.22–1.31	1.45	1.45	0.04
Ma9	13.0	90.2	Feb. 2077	1.29–1.33	1.31	1.31	0.04
Doc5	8.0	90.8	Oct. 2077	1.18–1.19	0.64	0.64	0.03
Ma8	8.3	62.9	Nov. 2049	1.17–1.19	0.60	0.60	0.05
Ma7	4.7	38.8	Oct. 2025	1.15–1.16	0.30	0.30	0.05
Doc6	3.4	38.8	Oct. 2025	1.13	0.21	0.21	0.03
Ma4	20.2	β_{avg} = 93% in year 2100		1.07	0.96	0.89	—
Ma3	3.3	β_{avg} = 93% in year 2100		0.98	0.03	0.02	—
Ma2	6.5	β_{avg} = 93% in year 2100		1.01	0.07	0.04	—
NMC-1	3.6	16.2	Mar. 2003	0.99	0.02	0.02	0.09
Ma1	9.0	16.2	Mar. 2003	1.02	0.05	0.05	0.22
Ma0	7.6	16.2	Mar. 2003	0.94	0.04	0.04	0.26
NMC-5	6.6	16.2	Mar. 2003	0.93	0.05	0.05	0.28
				$\sum$	15.76	15.66	1.98

Note: EOP compression calculated from EOP void ratio for Ma4 through Ma2.
[a]EOP compression corresponds to β_{avg} = 95% for Ma13 through Doc6 and NMC-1 through NMC-5.

Acknowledgments

The authors gratefully acknowledge Mr. Naoki Nishimura for providing settlement and pore-water pressure observations at MP2-II and Mr. Hiroyuki Tanaka for providing laboratory oedometer data for Osaka Bay Pleistocene clays. Additionally, the authors acknowledge Mr. Yoshiyuki Morikawa, Mr. Masaki Kobayashi, and Mr. Mamoru Mimura for useful email communications regarding the Kansai Airport project.

Notation

The following symbols and abbreviations are used in this paper:

A_c = activity;
C_c = compression index;
C'_c = secant compression index;
C_k = change in permeability index;
C_r = recompression index;
C_α = secondary compression index;
e = void ratio;
e_o = initial or preconstruction void ratio;
e_p = end of primary void ratio;
G_s = specific gravity of solids;
I_p = plasticity index;
k_{vo} = initial or prereclamation coefficient of permeability in the vertical direction;
L_o = initial layer thickness;
t_p = time to end of primary consolidation;
u' = excess pore-water pressure;
w_o = natural or prereclamation water content;
w_p = plastic limit;
w_l = liquid limit;
γ = total unit weight;
γ_w = unit weight of water;
$\Delta\sigma_v$ = increase in vertical stress;
$\dot{\varepsilon}_I$ = imposed strain rate for CRS test;
$\dot{\varepsilon}_p$ = imposed strain rate for CRS test that produces the EOP e-log σ'_v relationship;
σ'_p = preconsolidation pressure;
σ'_v = effective vertical stress; and
σ'_{vo} = initial or prereclamation effective vertical stress.

References

Akai, K., and Tanaka, Y. (1999). "Settlement behaviour of an off-shore airport KIA." *Geotechnical engineering for transportation infrastructure*, F. B. J. Barends, J. Lindenberg, H. J. Luger, A. Verruijt, and L. de Quelerij, eds., Taylor & Francis, Tokyo, 1041–1046.

Arai, Y. (1991). "Construction of an artificial offshore island for the Kansai International Airport." *Proc., GEO-COAST '91: Int. Conf. on Geotechnical Engineering for Coastal Development: Theory and Practice on Soft Ground*, Coastal Development Institute of Technology, Yokohama, Japan, 927–943.

Endo, H., Oikawa, K., and Komatsu, A. (1991). "Settlement of diluvial clay layers caused by a large scale man-made island." *Proc., GEO-COAST '91: Int. Conf. on Geotechnical Engineering for Coastal Development, Coastal Development Institute of Technology: Theory and Practice on Soft Ground*, Coastal Development Institute of Technology, Yokohama, Japan, 177–182.

Funk, J. R. (2013). "Settlement of the Kansai International Airport Islands." Ph.D. thesis, Univ. of Illinois at Urbana–Champaign, Urbana, IL.

Funk, J. R., and Mesri, G. (2014). *ILLICON user guide*, Department of Civil and Environmental Engineering, Univ. of Illinois at Urbana–Champaign, Urbana, IL.

Furudoi, T. (2010). "The second phase construction of Kansai International Airport considering the large and long-term settlement of the clay deposits." *Soils Found.*, 50(6), 805–816.

Furudoi, T., and Kobayashi, M. (2009). "Geotechnical issues and approach on Kansai International Airport Project—Prediction and performance of settlement." *J. Soc. Civ. Eng. Ser. C*, 65(4), 998–1017.

Hight, D. W., and Leroueil, S. (2003). "Characterisation of soils for engineering purposes." *Characterisation and engineering properties of natural soils*, T. S. Tan, K. K. Phoon, D. W. Hight, and S. Leroueil, eds., Vol. 1, Swets & Zeitlinger, Lisse, Netherlands, 255–362.

Imai, G., Ohmukai, N., and Tanaka, H. (2005). "An isotaches-type compression model for predicting long term consolidation of KIA clays." *Proc., Symp. on Geotechnical Aspects of Kansai International Airport*, Port and Harbor Institute, Yokosuka, Japan, 49–64.

Inoue, N., Kitada, N., Itoh, Y., Takemura, K., and Nakagawa, K. (2003). "Integrated study of high resolution geophysical and geological information of Osaka Bay, Southwest Japan." *J. Asian Earth Sci.*, 22(1), 1–11.

Itihara, M., Yoshikawa, S., Inoue, K., Hayashi, T., Tateishi, M., and Nakajima, K. (1975). "Stratigraphy of the Plio-Pleistocene Osaka Group in Sennan-Senpoku area, south of Osaka, Japan—A standard stratigraphy of the Osaka Group." *J. Geosci. Osaka City Univ.*, 19, 1–29.

Itoh, Y., Takemura, K., Ishiyama, T., Tanaka, Y., and Iwaki, H. (2000). "Basin formation at a contractional bend of a large transcurrent fault: Plio-Pleistocene subsidence of the Kobe and northern Osaka Basins, Japan." *Tectonophysics*, 321(3), 327–341.

Itoh, Y., Takemura, K., Kawabata, D., Tanaka, Y., and Nakaseko, K. (2001). "Quaternary tectonic warping and strata formation in the southern Osaka Basin inferred from reflection seismic interpretation and borehole sequence." *J. Asian Earth Sci.*, 20(1), 45–58.

Jeon, B., Mimura, M., and Saitsu, Y. (2012). "Numerical assessment of the permeability for the Pleistocene sandy gravel deposits considering the subsurface stratigraphy of Kansai International Airport." Disaster Prevention Research Institute, Kyoto Univ., Kyoto, Japan, 215–224.

Kagawa, T., Zhao, B., Miyakoshi, K., and Irikura, K. (2004). "Modeling of 3D basin structures for seismic wave simulations based on available information on the target area: case study of the Osaka Basin, Japan." *Bull. Seismol. Soc. Am.*, 94(4), 1353–1368.

Kanda, K., Suzuki, S., and Yamagata, N. (1991). "Offshore investigation at the Kansai International Airport." *Proc., GEO-COAST '91: Int. Conf. on Geotechnical Engineering for Coastal Development: Theory and Practice on Soft Ground*, Coastal Development Institute of Technology, Yokohama, Japan, 33–38.

Kansai International Airport Land Development Company (KALD). (2005). *2nd phase construction in progress: Final stage of reclamation and background of the Kansai International Airport: Environmentally-friendly air traffic gateway to the world* (DVD-ROM), Yokohama, Japan.

Kobayashi, M., Furudoi, T., Suzuki, S., and Watabe, Y. (2005). "Modeling of consolidation characteristics of clays for settlement prediction of Kansai International Airport." *Proc., Symp. on Geotechnical Aspects of Kansai International Airport*, Japanese Geotechnical Society, Tokyo, 65–76.

Maeda, S., Higuchi, Y., and Furuichi, M. (1990). "Large-scale sand drain works for the Kansai International Airport." *Proc., Airports into the 21st Century*, Hong Kong Institute of Engineers, Hong Kong, 485–496.

Mesri, G. (2001). "Primary compression and secondary compression." *Proc., Soil Behavior and Soft Ground Construction*, Geotechnical special publication 119, J. T. Germain, T. C. Sheahan, and R.V. Whitman, eds., ASCE, Reston, VA, 122–166.

Mesri, G., and Ajlouni, M. (2007). "Engineering properties of fibrous peats." *J. Geotech. Geoenviron. Eng.*, 10.1061/(ASCE)1090-0241(2007)133:7(850), 850–866.

Mesri, G., and Castro, A. (1987). "C_α/C_c concept and K_0 during secondary compression." *J. Geotech. Engrg.*, 10.1061/(ASCE)0733-9410(1987)113:3(230), 230–247.

Mesri, G., and Choi, Y. K. (1979). "Discussion: Strain rate behavior of Saint-Jean Vianney clay, by Vaid et al." *Can. Geotech. J.*, 16(4), 831–834.

Mesri, G., and Choi, Y. K. (1985a). "Settlement analysis of embankments on soft clays." *J. Geotech. Engrg.*, 10.1061/(ASCE)0733-9410(1985)111:4(441), 441–464.

Mesri, G., and Choi, Y. K. (1985b). "The uniqueness of the End-Of-Primary (EOP) void ratio-effective stress relationship." *Proc., 11th Int. Conf. on Soil Mechanics and Foundation Engineering*, Vol. 2, Balkema, Rotterdam, Netherlands, 587–590.

Mesri, G., and Feng, T. W. (1986). "Discussion: Stress-strain-strain rate relation for the compressibility of sensitive natural clays, by Leroueil et al." *Géotechnique*, 36(2), 283–290.

Mesri, G., Feng, T. W., Ali, S., and Hayat, T. M. (1994). "Permeability characteristics of soft clays." *Proc., 13th Int. Conf. on Soil Mechanics and Foundation Engineering*, Vol. 2, Japanese Society of Soil Mechanics and Foundation Engineering, Tokyo, 187–192.

Mesri, G., Feng, T. W., and Shahien, M. (1995). "Compressibility parameters during primary consolidation. Invited special lecture." *Proc., Int. Symp. on Compression and Consolidation of Clayey Soils*, Balkema, Rotterdam, Netherlands, 201–217.

Mesri, G., and Godlewski, P. M. (1977). "Time and stress compressibility interrelationship." *J. Geotech. Engrg. Div.*, 103(5), 417–430.

Mesri, G., and Godlewski, P. M. (1979). "Time and stress-compressibility interrelationships. Closure." *J. Geotech. Engrg. Div.*, 105(1), 106–113.

Mesri, G., and Khan, A. Q. (2012). "Ground improvement using vacuum loading together with vertical drains." *J. Geotech. Geoenviron. Eng.*, 10.1061/(ASCE)GT.1943-5606.0000640, 680–689.

Mikasa, M., and Ohnishi, H. (1981). "Soil improvement by dewatering in Osaka South Port." *Proc., 9th Int. Conf. on Soil Mechanics and Foundation Engineering: The Case History Volume*, International Society of Soil Mechanics and Foundation Engineering, Tokyo, 639–684.

Mimura, M., and Jang, W. (2005). "Long-term settlement of the Pleistocene deposits due to construction of KIA." *Proc., Symp. on Geotechnical Aspects of Kansai International Airport*, Japanese Geotechnical Society, Tokyo, 77–85.

Nakase, A. (1987). "Kansai International Airport—Construction of man-made island." *Proc., 8th Asian Regional Conference of International Society of Soil Mechanics and Foundation Engineering*, Vol. 2, International Society of Soil Mechanics and Foundation Engineering, London, 87–101.

Nakaseko, K., Takemura, K., Nishiwaki, N., Nakagawa, Y., Furutani, M., and Yamauchi, M. (1984). "Stratigraphy of the submarine strata at the Kansai International Airport in Osaka Bay off Senshu, central Japan." *Rep. of the Calamity Science Institute*, K. Nakaseko, ed., Osaka, Japan, 191–198.

New Kansai International Airport Company (NKIAC). (2012). ⟨http://www.nkiac.co.jp⟩ (Oct. 22, 2012).

Rocchi, G., Vaciago, G., Fontana, M., and Plebani, F. (2006). "Enhanced prediction of settlement in structured clays with examples from Osaka Bay." *Geomech. Geoeng.*, 1(3), 217–237.

Rocchi, G., Vaciago, G., Fontana, M., and Plebani, F. (2007). "Further insight into the behavior of Pleistocene Osaka clays at KIA Phase 1 island." *Geomech. Geoeng.*, 2(3), 159–173.

Sasaki, S., Nakamura, Y., and Tokuhira, T. (1987). "Long-term goals of Osaka Port Improvement Project." *Proc., Coastal Zone '87: 5th Symp. on Coastal and Ocean Management*, O. T. Magoon, H. Converse, D. Miner, L. T. Tobin, D. Clark, and G. Domurat, eds., Vol. 1, ASCE, Reston, VA, 267–274.

Sekiguch, H., and Aksornkoae, S. (2008). "Environment problems in the coastal zone." *Asia-Pacific coasts and their management: States of environment*, N. Mimura, ed., Springer, Dordrecht, Netherlands, 65–171.

Shibata, T., and Karube, D. (2005). "Settlement prediction of Kansai International Airport." *Proc., 16th Int. Conf. on Soil Mechanics and Geotechnical Engineering*, IOS Press, Amsterdam, Netherlands, 87–96.

Shinohara, M. (2003). "Settlement analysis and intelligent site management of the second-phase land reclamation works for Kansai International Airport." *Proc., Nakase Memorial Symposium Yokosuka, Japan: Soft Ground Engineering in Coastal Areas*, Balkema, Rotterdam, Netherlands, 145–150.

Tabata, T., and Morikawa, Y. (2005). "The second phase construction of Kansai International Airport considering the large and long-term settlement of the clay deposits." *Proc., Int. Conf. on Soil Mechanics and Geotechnical Engineering*, IOS Press, Amsterdam, Netherlands, 7–16.

Tanaka, H. (2005a). "Consolidation behavior of natural soils around p_c value—Inter-connected oedometer test." *Soils Found.*, 45(3), 97–105.

Tanaka, H. (2005b). "Consolidation behavior of natural soils around p_c value—Long term consolidation test." *Soils Found.*, 45(3), 83–95.

Tanaka, H., Kang, M., and Watabe, Y. (2004). "Ageing effects on consolidation properties: Based on the site investigation of Osaka Pleistocene clays." *Soils Found.*, 44(6), 39–51.

Tanaka, H., and Locat, J. (1999). "A microstructural investigation of Osaka Bay clay: The impact of microfossils on its mechanical behaviour." *Can. Geotech. J.*, 36(3), 493–508.

Tanaka, H., Tanaka, M., Suzuki, S., and Sakagami, T. (2003). "Development of a new cone penetrometer and its application to great depths of Pleistocene clays." *Soils Found.*, 43(6), 51–61.

Tavenas, F., Jean, P., Leblond, P., and Leroueil, S. (1983). "The permeability of natural soft clays. Part II: Permeability characteristics." *Can. Geotech. J.*, 20(4), 645–660.

Terzaghi, K., Peck, R. B., and Mesri, G. (1996). *Soil mechanics in engineering practice*, 3rd Ed., Wiley, New York.

Tsuchida, T. (2005). "Structure due to cementation of Osaka Bay clay and its mathematical modeling." *Proc., Symp. on Geotechnical Aspects of Kansai International Airport*, IOS Press, Amsterdam, Netherlands, 31–40.

Watabe, Y., Tsuchida, T., and Adachi, K. (2002). "Undrained shear strength of Pleistocene clay in Osaka Bay." *J. Geotech. Geoenviron. Eng.*, 10.1061/(ASCE)1090-0241(2002)128:3(216), 216–226.

Watabe, Y., Udaka, K., and Morikawa, Y. (2008). "Strain rate effect on long-term consolidation of Osaka Bay clay." *Soils Found.*, 48(4), 495–509.

Yamane, N., Fukasawa, T., and Mizukami, J. (2003). "A new construction method for reclamation work in the Kansai International Airport second phase project." *Proc., Nakase Memorial Symposium, Yokosuka, Japan: Soft Ground Engineering in Coastal Areas*." Balkema, Rotterdam, Netherlands, 201–204.

Yamasaki, T., and Nakada, M. (1996). "Effects of quaternary sea-level change on the subsidence of a sedimentary basin: A case study of the Osaka Bay sedimentary basin, Japan." *Tectonophysics*, 267(1–4), 229–238.